Amplitude and AVO response of a single thin bed

Yinbin Liu and Douglas R. Schmitt, Department of Physics, University of Alberta, T6G 2J1, Canada

Summary

The reflection amplitude and AVO responses of thin layers are numerically studied by propagator matrix method. The results show that the influence of an extra-thin bed ($\lambda/d > 4$) on reflection amplitude and AVO is great for opposite polarity reflections and is small for identical polarity reflections. For opposite polarity reflections, the maximum absolute amplitude of reflection signal versus wavelength/thickness exhibits a "S" form of character for the under-critical incidence and monotonously decreases from near 1 to zero for the over-critical angle incidence. The reflection amplitudes are proportional to the thickness of thin layer. For identical polarity reflections, the maximum absolute amplitude of reflection signal versus wavelength/thickness exhibits a "V" form of character for the under-critical incidence and has near 1 reflection amplitudes for the over-critical angle incidence. The reflection amplitudes are inversely proportional to the thickness of thin layer. The AVO responses for two kinds of reflections gradually increase with increasing angle of the incident angle.

Introduction

An extra-thin gas sand layer can often have a detectable seismic reflection response. Generally, the reflections from thin layer are concerned with seismic resolution, detection, and amplitude variation with angle or offset (AVO). Resolution and detectability for a thin-layer have been studied by Widess (1973), Koefoed and de Woogd (1980), Kalweit and Wood (1982), de Voogd and Rooijen (1983), Gochioco (1991), Chung and Lawton (1995, 1996), and others.

In exploration geophysics the generally acceptable threshold for vertical resolution is a quarter of the dominant wavelength (Yilmaz, 1987). In this paper the layer is called as thin layer when $1 < \lambda_2/d <$ about 4 and extra-thin layer when $\lambda_2/d >$ about 4, where λ_2 is the wavelength within the layer. We will focus our discussion on the amplitude and AVO responses for an extra-thin bed.

Widess' approach (1973) as well as its extensions (Koefoed and de Woogd, 1980; Kalweit and Wood, 1982; de Voogd and Rooijen, 1983; Gochioco, 1991; Chung and Lawton, 1995; 1996) are useful in the study of seismic resolution. However, they do not properly provide the amplitude responses from an extra-thin layer because elastic waves propagated in the layer are coupled P and SV waves subject to a structural frequency dispersion (generalized Lamb's waves). The delay time transmission/reflection method for AVO (e.g., Juhlin and Yong, 1993) is based on plane wave ray theory and so is not able to study the case for the over-critical angle incidence. In this paper, the amplitude and AVO responses of a thin or extra-thin bed are quantitatively studied by a propagator matrix method that provides an exact solution.

Theory and algorithm

Method The model consists a thin layer embedded between two half spaces (Figure 1). The reflection pressure field can be derived by propagator matrix approach (Liu and Schmitt, 2001). This method is an exact solution for either acoustic or elastic media and so contains all multiple and converted or coupled waves within the layer.

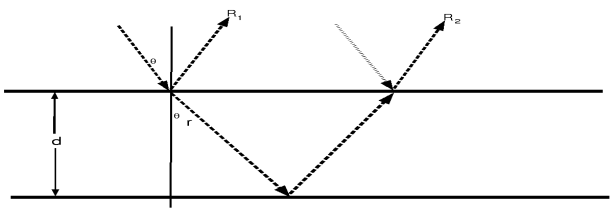

Fig. 1. Thin bed model and reflection ray. The time delay δt for R_1 and R_2 is $2d\cos\theta_r/v_2$.

Table 1. Parameters for three models

	Model I	Model II	Model III
$v_1(m/s)$	2200	3050	3050
$\rho_1(g/cm^3)$	2.3	2.7	2.7
$v_2(m/s)$	1500	6100	4575
$\rho_2(g/c^3)$	2.2	2.7	2.7
$v_3(m/s)$	2500	3050	6100
$\rho_3(g/cm^3)$	2.35	2.7	2.7

Model Three different models are described in Table 1. The corresponding shear wave velocities are calculated by taking Possion's ratio $\sigma = 0.25$. Model I is representation of the Wabasca gas formation in northern Alberta (Schmitt, 1999), model II is Widess' calculated parameters and model III denotes the transition layers. The densities for models II and III are uniform. Models I and II are opposite polarity P-wave reflections and model III is identical polarity P-wave reflections. The opposite (identical) polarity reflections mean that wavelet reflections from the top and bottom of a thin layer are opposite (identical) polarity. Generally, a high or low velocity bed

($\rho_2 v_2 > \rho_1 v_1$ and $\rho_3 v_3$ or $\rho_2 v_2 < \rho_1 v_1$ and $\rho_3 v_3$) is opposite polarity reflections and a increased or decreased velocity bed ($\rho_1 v_1 > \rho_2 v_2 > v_3 \rho_3$ or $\rho_1 v_1 < \rho_2 v_2 < v_3 \rho_3$) is identical polarity reflections.

To study the influence of the SV wave on reflection amplitude we compare the pressure field from both acoustic (i.e, no shear wave) and elastic thin layer reflections. Figures 2 shows the calculated reflection waveforms of model I for a 50-Hz Ricker wavelet incidence when the top is acoustic half-space and the thin layer and bottom half-space are elastic with Poisson's ratio $\sigma = 0.25$ (solid) and when the thin layer and two half spaces are all acoustic (dash) at $\theta = 20^0$. It can be seen that the amplitude responses for elastic layer are basically similar to those for acoustic layer except with a little smaller amplitude. This is because in the elastic case part of the energy converts into shear waves or Lamb waves and radiates into the bottom half-space. As reported by Juhlin and Young (1993), the interbed S-waves and interbed P-S conversions are negligible when the contrast in elastic properties between the thin layer and surrounding media is small. In the following analysis we will neglect the influence of SV waves.

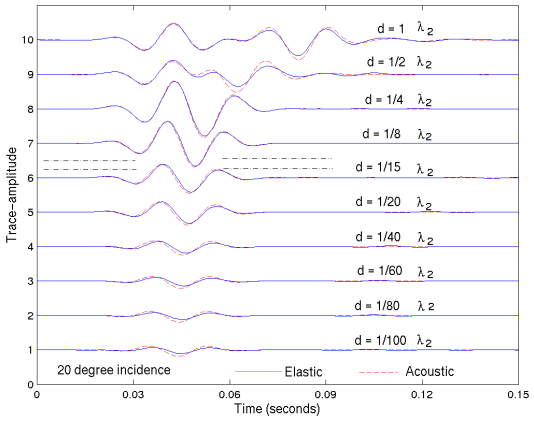

Fig. 2. Comparison between elastic (Poisson's ratio $\sigma = 0.25$) and acoustic thin layers in model I for a 50-Hz Ricker wavelet incidence for the thickness of thin layers from $d = \lambda_2$ to $d = 1/100\,\lambda_2$. Solid and dash lines denote the elastic and acoustic layers, respectively.

Effects of Bed Thickness and Incident Angle on Reflection Amplitude

Opposite polarity reflection Figure 3 is the reflection composite waveforms of model II calculated by propagator matrix method for a 50-Hz Ricker wavelet at normal (solid) and $\theta = 20^0$ (dash) incidences for $d = \lambda_2$ to $d = 1/8\,\lambda_2$ (Figure 3a) and $d = 10\lambda_2$ to $d = 1/100\,\lambda_2$ (Figure 3b). The waveforms for normal incidence are similar to those of Widess (1973) computed by time delay approximation. It can be seen that two reflection wavelets from the top and bottom of thin bed overlap, the time delay δt for R_1 and R_2 depends on the incident angle and the material properties and can be approximately calculated by ray theory, which is equal to $2d\cos\theta_r / v_2$, where θ_r is refracted angle and v_2 is P-wave velocity of the layer (Juhlin and Young, 1993). Either the thinner the bed or the larger the refracted angle, the smaller the delay time δt and so the more the overlap. The influence of an extra-thin bed on reflection amplitudes is great for opposite polarity reflections. For example, the reflection amplitudes are about 20% ($\theta = 0^0$) and 22% ($\theta = 20^0$) of the amplitude of the incident wave for $\lambda_2 / d = 20$. A bed with $\lambda_2 / d = 40$ still has about 11% ($\theta = 0^0$ and 20^0) of the amplitude of the incident wave.

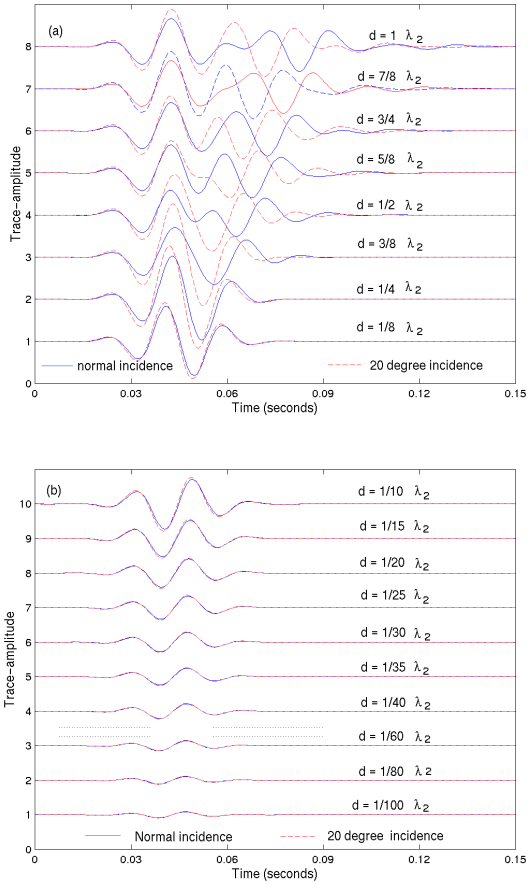

Fig. 3. Opposite polarity reflections for a 50-Hz plane Ricker wavelet incidence (model II). Solid and dash lines denote the normal and $\theta = 20^0$ incidences, respectively. (a) the thickness of thin layers from $d = \lambda_2$ to $d = 1/8\,\lambda_2$; (b) the thickness of extra-thin layers from $d = 1/10\,\lambda_2$ to $d = 1/100\,\lambda_2$.

Figure 4 shows the maximum absolute amplitudes as a function of wavelength/thickness (λ_2 / d) for several incident angles. It can be seen that the amplitude responses for opposite polarity reflections exhibit a "S" form of character for the under-critical incidence ($\theta <$ critical angle $\theta_c = 30^0$), which first decrease from the amplitude of the single reflection wavelets to

a minimum at λ_2/d = about 2 for normal incidence (destructive interference) and then increase to a maximum at λ_2/d = about 4 for normal incidence (constructive interference) and finally gradually decrease to zero. The greater the incidence or the thickness of the extra-thin layer, the larger the reflection amplitudes. The minimums and maximums for the high angle of the incidence appear earlier than those for the low angle of the incidence because of the oblique incidence as if the layer were thicker. The maximum absolute amplitudes for the over-critical incidence ($\theta > 30^0$) gradually decrease from near 1 (completed reflection) to zero because in this case the wave within the thin layer is an inhomogeneous mode wave with complex wavenumber and result in the amplitude attenuation.

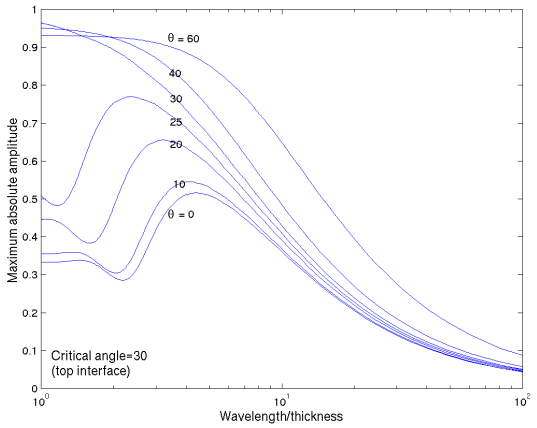

Fig. 4. Maximum absolute amplitudes of opposite polarity reflections (model II) as a function of d/λ_2 for several incident angles.

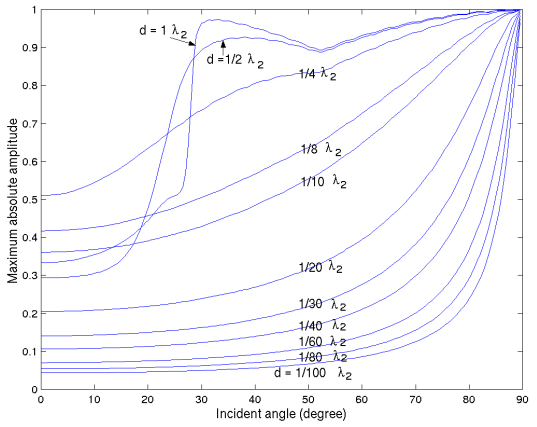

Fig. 5. Maximum absolute amplitude variation with angle or offset (AVO) of opposite polarity reflections for a 50-Hz Ricker wavelet incidence in different wavelength/thickness (d/λ_2) in model II.

Figure 5 shows the AVO response of a 50-Hz Ricker wavelet incidence for model II where thickness of the layer was varied from $d = \lambda_2$ to $d = 1/100\,\lambda_2$. The maximum absolute amplitudes or reflection coefficients increase with increasing angle of the incidence or offset but the change is very small when θ < about 40^0 for λ_2/d > 20, the influence of the critical angle of the top interface on reflection coefficients and AVO is obvious for λ_2/d < about 2 and can not be observed for λ_2/d > about 4. AVO response smoothly passes the critical angle ($\theta_c = 30^0$) and only near grazing incidence ($\theta \to 90^0 >> \theta_c$) has a near 1 value. This indicates that the reflection characteristics of an extra-thin layer are much different those of a single interface, the later has near 1 reflection amplitude for the over-critical angle incidence.

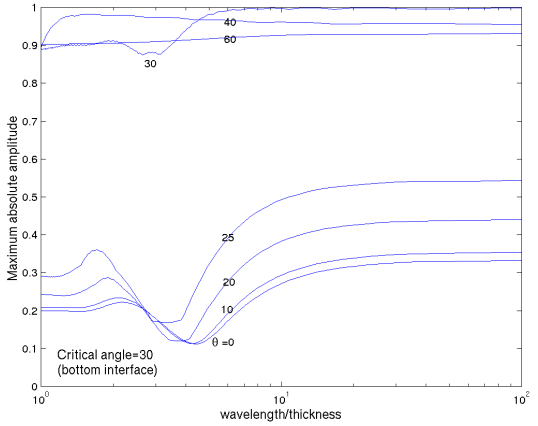

Fig. 6. Maximum absolute amplitudes of identical polarity reflections (model III) as a function of d/λ_2 for several incident angles.

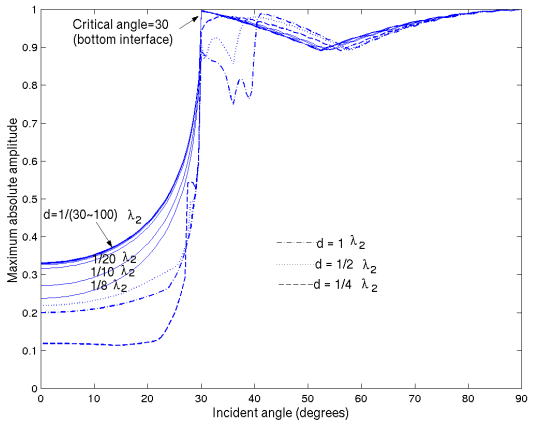

Fig. 7. Maximum absolute amplitude variation with angle or offset (AVO) of identical polarity reflections for a 50-Hz Ricker wavelet incidence in different wavelength/thickness (d/λ_2) in model III.

Identical polarity reflection Figure 6 shows the maximum absolute amplitudes for the Ricker wavelet incidence as a function of wavelength/thickness for several incident angles. Figure 7 is the AVO response for the Ricker wavelet incidence for $d = \lambda_2$ to $d = 1/100\,\lambda_2$. The amplitude responses for identical polarity reflection exhibit a "V" form of character for the

under-critical incidence ($\theta < \theta_c = 30^0$,bottom interface), which first increase from the amplitude of the single reflection wavelets to a maximum at λ_2/d = about 2 for normal incidence (constructive interference) and then decrease to a minimum at λ_2/d = about 4 for normal incidence (destructive interference) and finally increase to the amplitude of the single bottom reflection wavelet (without thin layer), the maximums and minimum shift to smaller values of λ_2/d for the high angle of the incidence. It can be seen from Figures 6 and 7 that the smaller the thickness, the larger the reflection amplitude for the under-critical incidence because of the effect of transition layer reflections. The maximum absolute amplitudes for $\lambda_2/d >$ about 20 are basically invariable with the wavelength/thickness ratio, this means that the amplitude differences with and without thin layers are small, so the amplitude responses of identical polarity reflections are not sensitive to an extra-thin layer. The maximum absolute amplitudes for the over-critical incidence for identical polarity reflections are near 1, which is similar to the completed reflection from a single interface.

Conclusions

The amplitude and AVO responses of a thin or extra-thin bed with either identical or opposite polarity reflections are numerically studied by propagator matrix method. The influence of an extra-thin bed on reflection amplitudes is strong for opposite polarity reflections and is weak for identical polarity reflection. For opposite polarity reflections, the amplitude versus wavelength/thickness exhibits a "S" form of character for the under-critical incidence and monotonously decreases for the over-critical angle incidence. The reflection amplitude is proportional to the thickness of extra-thin layer. For identical polarity reflections, the amplitude versus wavelength/thickness exhibits a "V" form of character and is basically invariant for $\lambda_2/d > 20$ for the under-critical angle incidence and has near 1 reflection amplitude for the over-critical angle incidence. The reflection amplitude is inversely proportional to the thickness of extra-thin layer. The AVO responses for two kinds of cases gradually increase with increasing angle of the incident angle.

Acknowledgements

The authors thank Mr. Guoping Li, PanCanadian, for his suggestion on thin layer seismic attributes. This work sponsored by the Consortium Project on Seismic Heavy Oil in Department of Physics, University of Alberta.

References

Chung, H. M. & D. C. Lawton, 1995, Amplitude responses of thin beds: Sinusoidal approximation versus Ricker approximation, Geophysics, 60, 223-230.

Chung, H. M. & D. C. Lawton, 1996, Frequency characteristics of seismic reflections from thin beds, Can. J. Expl. Geophys., 31, 32-37.

de Voogd, N. & den Rooijen H., 1983, Thin-layer response and spectral bandwidth, Geophysics, 48, 12-18.

Gochioco, L. M., 1991, Tuning effect and interference reflections from thin beds and coal seams, Geophysics, 56, 1228-1295.

Juhlin C. & R. Young, 1993, Implication of thin layers for amplitude variation with offset (AVO) studies, Geophysics, 58, 1200-1204.

Kallweit R. S. & L. C. Wood, 1982, The limits of resolution of zero-phase wavelets, Geophysics, 47, 1035-1046.

Koefoed O. & N. de Voogd, 1980, The linear properties of thin layers, with an application to synthetic seismograms over coal seams, Geophysics, 45, 1254-1268.

Liu Y. & D. R. Schmitt, 2001, Quntitative analysis of thin layer effects: The equivalent medium, SV-wave degeneracy and the transition between ray-theoretical and equivalent media, for submission to Geophys. J. Int.

Schmitt, D. R., 1999, Seismic attributes for monitoring of a shallow heated heavy oil reservoir: A case study, Geophysics, 64, 368-377.

Widess, M. B., 1973, How thin is a thin bed? Geophysics, 38,1176-1180.

Yilmaz, O, 1987, Seismic data processing, Society Exploration Geophysics.